SUPPORTING INFORMATION

A litmus test for the balanced description of dispersion interactions and coordination chemistry of lanthanoids

Juana Vázquez Quesada,*,† Jiří Chmela,† Jean-François Greisch,‡ Wim Klopper,†,‡ and Michael E. Harding*,‡

†*Institut für Physikalische Chemie, Karlsruher Institut für Technologie (KIT), Campus Süd, Postfach 6980, D-76049 Karlsruhe, Germany*

‡*Institut für Nanotechnologie, Karlsruher Institut für Technologie (KIT), Campus Nord, Postfach 3640, D-76021 Karlsruhe, Germany*

E-mail: juana.quesada@kit.edu; michael.harding@kit.edu

Abstract

The influence of long-range interactions on the structure of complexes of Eu(III) with four 9-hydroxy-phenalen-1-one ligands (HPLN) and one alkaline earth metal dication $[Eu(PLN)_4AE]^+$ (AE: Mg, Ca, Sr, and Ba) is analyzed. Through the $[Eu(PLN)_4Ca]^+$ complex, which is a charged complex with two metals—one of them a lanthanoid—and with four relative fluxional π-ligands, the difficulties of describing such systems are identified. The inclusion of the D3(BJ) or D4 corrections to different density functionals introduces significant changes in the structure, which are shown to stem from the interaction between pairs of PLN

ligands. This interaction is studied further with a variety of density functionals, wave-function based methods, and by means of the random phase approximation. By comparing the computed results with those from experimental evidence of gas-phase photoluminescence and ion mobility measurements it is concluded that the inclusion of dispersion corrections does not always yield structures that are in agreement with the experimental findings.

I. Structures and Energy of series $[Eu(PLN)_4AE]^+$

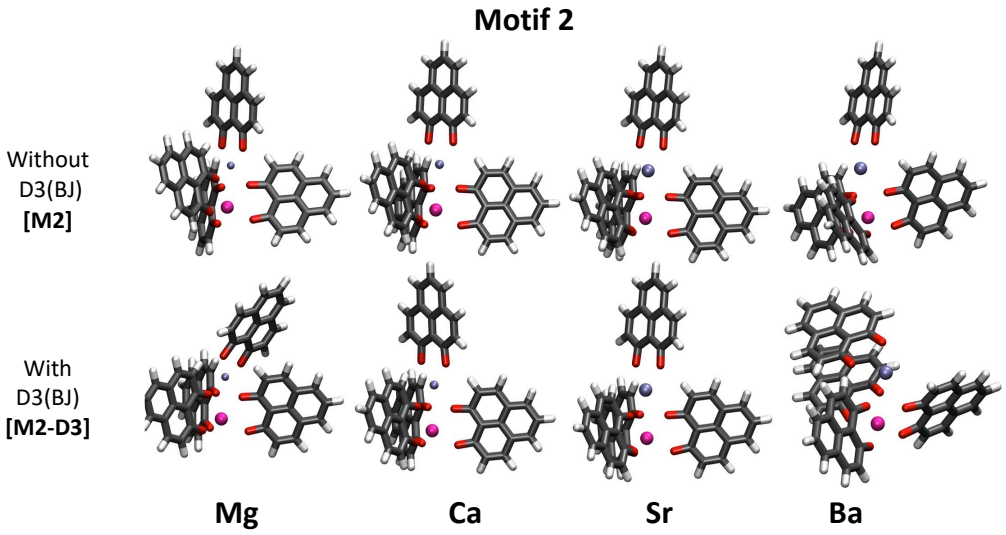

Figure 1: Structures of $[Eu(PLN)_4AE]^+$ (AE = Mg, Ca, Sr, and Ba) computed at the BP86/def2-TZVPP level of theory for motif 2 Ref. 1) with (M2-D3) and without (M2) dispersion correction D3(BJ) (europium: pink; AE: purple; oxygen: red).

Energetically, the motif 1 [M1-D3] structures are considerably more stable than their motif 2 [M2-D3] counterparts (Table 1) suggesting that the formation of the stacked PLN pair is associated with a significant attraction energy gain. The new results were compared with

Table 1: Energy differences (in kJ mol^{-1}) for motif 1 [M1] and motif 2 [M2] including the zero-point energy correction for different complexes computed at the BP86/def2-TZVPP level of theory with and without dispersion corrections of the type D3(BJ).

Complex	$(E_{M2} - E_{M1})$	$(E_{M2\text{-}D3(BJ)} - E_{M1\text{-}D3(BJ)})$
$[Eu(PLN)_4Mg]^+$	8[a]	40
$[Eu(PLN)_4Ca]^+$	−7[a]	45
$[Eu(PLN)_4Sr]^+$	−9[a]	53
$[Eu(PLN)_4Ba]^+$	−9[a]	34

[a] Data taken from Ref. 1.

the experimental information from the photoluminescence spectrum and the cross section values obtained from ion mobility measurements. At this point we want to mention that the

photoluminescence spectrum for the complex with Ba ($[Eu(PLN)_4Ba]^+$) was experimentally inaccessible and that the theoretical results for the $^5D_0 \rightarrow {}^7F_2$ band were computed using ligand field theory. The calculated and experimental transition energies are shown in Figure 2. The latter are presented in terms of a contour map reporting transition energies and relative intensities as one. Identical amplitudes for the transitions of the $^5D_0 \rightarrow {}^7F_2$ band have been assumed. The experimental broadening was resembled using Gaussian functions, whose widths are consistent with the experimental resolution and whose superpositions provide the maxima displayed. In Figure 2, it can be observed that in the case of motif 2, whose structures with [M2-D3] and without [M2] dispersion corrections are very similar, the spectrum follows the experimental trend. In the case of motif 1, however, only the structures obtained at the BP86/def2-TZVPP level [M1] are in good agreement with the experiment. In the case of the stacked configuration obtained after considering dispersion forces by means of the model D3(BJ) [M1-D3], the profile—split into three components—and the energies of the transitions differ considerably from the experimental pattern.

The comparison of the He-converted cross-section of all the structures computationally suggested, that is, M1, M1-D3, M2, and M2-D3, as well as the experimental cross-sections for the complexes with Mg, Ca and Sr are presented in Figure 3. In view of the results, the M1-D3 structures can be ruled out since they differ considerably from the experimental evidence. The other three structures are indistinguishable considering the current experimental resolution. Thus, although the M1-D3 structures are energetically the most stable, they poorly agree with experiment showing that they are not present in the gas-phase measurements. This is consistent with a previous study from which it turned out that D3(BJ) in conjunction with the BP86 functional is inferior compared to D2 with an increase of the mean absolute deviation (MAD) of +24 kcal mol^{-1} in comparison with its predecessor D model and considering different test sets and basis sets.[2]

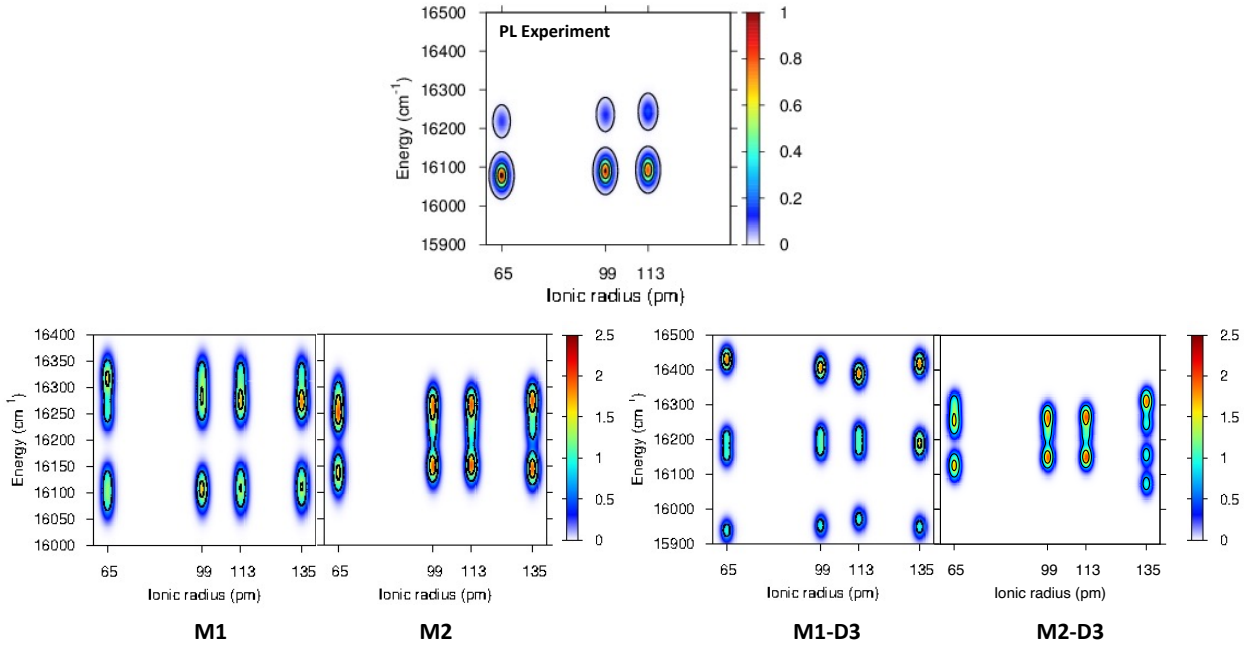

Figure 2: Experimental band positions and relative intensities for the $^5D_0 \rightarrow {}^7F_2$ transitions of $[Eu(PNL)_4AE]^+$ (AE = Mg, Ca, and Sr) (PL experiment) as well as computed transitions, including $[Eu(PNL)_4Ba]^+$, from the $^5D_0$ level to the split $^7F_2$ level manifolds for motifs 1 and 2 with (M1-D3 and M2-D3) and without (M1 and M2) dispersion corrections [D3(BJ)] (ionic radius: Mg = 65; Ca = 99; Sr = 113; Ba = 135 pm).

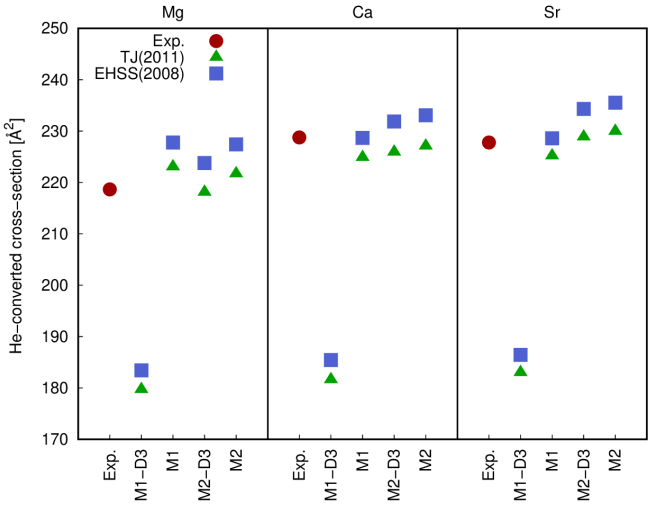

Figure 3: Experimental and calculated He-converted cross-sections for $[Eu(PNL)_4AE]^+$ with AE = Mg, Ca, and Sr. Calculated values correspond to motif 1 and 2 with geometries obtained at the BP86/def2-TZVPP level of theory with (M1-D3 and M2-D3) and without (M1 and M2) dispersion corrections [D3(BJ)]. The blue squares and the green triangles represent two different methods of calculating the cross-sections, the exact hard-spheres scattering (EHSS) model[3] and the trajectory model,[4] respectively.

II. Reference Cartesian coordinates

Starting-point configurations used for the geometry optimization of [Eu(PNL)$_4$Ca$^+$] complex (Ångström).

[Eu(PNL)$_4$Ca] $^+$	(M1)						BP86/def2-TZVPP
Eu	0.10011	-0.52036	0.17429	O	-0.96827	1.06553	-1.35406
Ca	0.30443	2.81510	-0.43307	C	3.33282	-1.00139	1.00970
C	-0.48621	-3.46133	-1.32342	C	4.19343	-1.87405	1.76248
C	-0.10449	-4.31087	-2.41892	H	3.70509	-2.63106	2.37493
H	0.60397	-3.89801	-3.13599	C	5.55317	-1.76967	1.69876
C	-0.61570	-5.57068	-2.55862	H	6.18275	-2.45350	2.27124
H	-0.31095	-6.19307	-3.40218	C	6.18596	-0.77751	0.88758
C	-1.55238	-6.10379	-1.62106	C	5.36736	0.12425	0.14022
C	-1.94885	-5.29301	-0.51311	C	3.93771	0.03332	0.19138
C	-1.41760	-3.97614	-0.34303	C	7.58694	-0.67297	0.82175
C	-2.08328	-7.39943	-1.76609	H	8.19177	-1.37123	1.40236
H	-1.76545	-8.00459	-2.61653	C	8.20573	0.30055	0.03589
C	-2.99914	-7.91125	-0.84765	H	9.29213	0.36470	-0.00348
H	-3.40085	-8.91539	-0.97577	C	7.42250	1.18961	-0.69282
C	-3.39760	-7.12902	0.23472	H	7.89244	1.95834	-1.30807
H	-4.11609	-7.51946	0.95704	C	6.01384	1.12156	-0.65200
C	-2.88819	-5.82911	0.42044	C	5.20587	2.03351	-1.38823
C	-3.29301	-5.01827	1.52315	H	5.69416	2.78927	-2.00595
H	-4.01515	-5.42567	2.23325	C	3.83921	1.97067	-1.33396
C	-2.79520	-3.75717	1.70236	H	3.23075	2.66073	-1.92083
H	-3.10099	-3.13939	2.54575	C	3.15455	0.98685	-0.54810
C	-1.83196	-3.19388	0.79820	C	0.33117	4.14939	2.58010
C	-1.33952	3.35884	-3.21295	C	0.64841	5.35384	3.30870
C	-1.60406	4.34827	-4.22807	H	1.06474	6.17441	2.72526
H	-1.05402	5.28493	-4.14292	C	0.42733	5.46646	4.64831
C	-2.50220	4.13291	-5.22997	H	0.67009	6.39393	5.17060
H	-2.68738	4.90484	-5.97950	C	-0.12822	4.38492	5.40265
C	-3.22583	2.90309	-5.32418	C	-0.44834	3.16464	4.72814
C	-2.98665	1.88419	-4.34932	C	-0.22168	3.01783	3.31925
C	-2.04041	2.08210	-3.28694	C	-0.35573	4.50704	6.78294
C	-4.15664	2.68948	-6.35480	H	-0.10118	5.44778	7.27360
H	-4.31813	3.48362	-7.08547	C	-0.89634	3.45518	7.52704
C	-4.86814	1.49220	-6.45558	H	-1.06726	3.57084	8.59638
H	-5.58669	1.34636	-7.26088	C	-1.21290	2.26191	6.88900
C	-4.64827	0.49016	-5.51778	H	-1.63591	1.43094	7.45550
H	-5.19509	-0.45189	-5.58132	C	-0.99717	2.09653	5.50417
C	-3.71987	0.66352	-4.46939	C	-1.32100	0.87633	4.84781
C	-3.49037	-0.36255	-3.51077	H	-1.74924	0.06157	5.43443
H	-4.05289	-1.29434	-3.59248	C	-1.10818	0.71779	3.50559
C	-2.58274	-0.19537	-2.50173	H	-1.37571	-0.21717	3.00943
H	-2.41340	-0.99107	-1.77625	C	-0.54838	1.76046	2.69611
C	-1.82202	1.00982	-2.34731	O	2.06345	-1.18667	1.09502
O	0.01283	-2.27255	-1.27486	O	1.84595	1.01667	-0.54388
O	-1.37781	-2.00812	1.05165	O	0.54521	4.13748	1.32083
O	-0.50490	3.65986	-2.29062	O	-0.37024	1.50687	1.42193

[Eu(PNL)$_4$Ca]$^+$ (M1-D3)							BP86-D3(BJ)/def2-TZVPP
Eu	-0.31592	-0.75726	0.72678	C	2.56369	-0.35022	2.32691
C	-0.77276	-2.51126	-2.01733	C	3.22391	-0.68550	3.55686
C	-0.43336	-2.58730	-3.41172	H	2.80855	-1.52145	4.11717
H	0.45438	-2.04176	-3.72658	C	4.29663	0.02380	4.01157
C	-1.21231	-3.27239	-4.29738	H	4.76304	-0.23239	4.96382
H	-0.95289	-3.29391	-5.35669	C	4.83588	1.11132	3.26120
C	-2.37942	-3.97415	-3.86845	C	4.23497	1.45211	2.01217
C	-2.72653	-3.95297	-2.48200	C	3.07839	0.75334	1.54016
C	-1.93669	-3.22734	-1.54186	C	5.93740	1.84376	3.73368
C	-3.18146	-4.68110	-4.77882	H	6.36898	1.57291	4.69775
H	-2.89867	-4.68397	-5.83187	C	6.47432	2.89890	2.99691
C	-4.31898	-5.36890	-4.35754	H	7.33064	3.45369	3.37688
H	-4.92768	-5.91373	-5.07736	C	5.91381	3.22816	1.76656
C	-4.66877	-5.35827	-3.00927	H	6.32986	4.04363	1.17373
H	-5.55340	-5.89743	-2.66796	C	4.80269	2.52565	1.26232
C	-3.89189	-4.66590	-2.06297	C	4.21692	2.86952	0.01121
C	-4.23898	-4.65774	-0.67861	H	4.66958	3.66730	-0.57918
H	-5.12284	-5.21321	-0.36026	C	3.09559	2.23142	-0.44011
C	-3.49118	-3.97462	0.23720	H	2.63952	2.49832	-1.39380
H	-3.75054	-3.96430	1.29488	C	2.45278	1.20506	0.32539
C	-2.32748	-3.22418	-0.14710	C	1.19092	3.83857	1.94196
C	-1.37835	1.07800	-3.30294	C	2.22776	4.81915	2.13549
C	-1.06759	0.97791	-4.70782	H	2.35035	5.55201	1.33938
H	-0.21661	1.55921	-5.06042	C	3.02702	4.81726	3.23865
C	-1.83314	0.23916	-5.56106	H	3.82283	5.55592	3.34592
H	-1.59152	0.20537	-6.62498	C	2.84526	3.85862	4.28190
C	-2.98109	-0.48220	-5.10287	C	1.80332	2.88982	4.15504
C	-3.28750	-0.46867	-3.70931	C	0.98723	2.83589	2.97837
C	-2.46284	0.24875	-2.78864	C	3.67047	3.86129	5.41712
C	-3.79625	-1.20188	-5.98969	H	4.46676	4.60362	5.48071
H	-3.54028	-1.20715	-7.05009	C	3.48721	2.93962	6.44873
C	-4.91968	-1.89860	-5.53777	H	4.13368	2.96002	7.32463
H	-5.54430	-2.44511	-6.24218	C	2.46143	2.00590	6.35349
C	-5.23116	-1.89383	-4.18408	H	2.29511	1.28740	7.15708
H	-6.09982	-2.44069	-3.81713	C	1.61885	1.96278	5.22548
C	-4.42756	-1.19995	-3.25649	C	0.57524	1.00086	5.12285
C	-4.72386	-1.20842	-1.86536	H	0.40912	0.31403	5.95397
H	-5.60329	-1.75186	-1.51865	C	-0.19700	0.92278	3.99841
C	-3.90172	-0.58271	-0.96715	H	-0.99311	0.18162	3.91566
H	-4.09541	-0.62344	0.10384	C	0.01917	1.77389	2.86355
C	-2.73156	0.12067	-1.38896	O	1.53896	-1.04977	1.98652
O	-0.02251	-1.79571	-1.25558	O	1.29804	0.77412	-0.10568
O	-1.69985	-2.57303	0.77374	O	0.50320	3.89664	0.86331
O	-0.72720	1.90837	-2.58499	O	-0.64953	1.49615	1.77693
O	-1.92901	0.58494	-0.45737	Ca	-0.47000	2.38503	-0.40983

III. Study of the $[In(PLN)_4Ca]^+$ complex

Table 2: Energy differences and structural description of geometries of $[In(PLN)_4Ca]^+$ optimized with different DFT functionals. Starting points are structures (M1) and (M1-D3) of motif 1 from the complex with Eu. The energies are given in kJ/mol. All computations were performed with the def2-TZVPP basis set.

Method	Starting point	Relative energy	Type of structure	Method	Starting point	Relative energy	Type of structure
BP86	M1	0	open–open	PBE0	M1	0	open–open
	M1-D3	0	open–open		M1-D3	0	open–open
BP86-D4	M1	0	half-stacked	PBE0-D4	M1	0	open–open
	M1-D3	−24	stacked		M1-D3	−8	half-stacked
BLYP	M1	0	open–open	B3LYP	M1	0	open–open
	M1-D3	0	open–open		M1-D3	0	open–open
BLYP-D4	M1	0	open–open	B3LYP-D4	M1	0	open–open
	M1-D3	−15	half-stacked		M1-D3	−14	half-stacked
PBE	M1	0	open–open	BHLYP	M1	0	open–open
	M1-D3	0	open–open		M1-D3	0	open–open
PBE-D4	M1	0	open–open	BHLYP-D4	M1	0	open–open
	M1-D3	−8	half-stacked		M1-D3	−9	half-stacked
TPSS	M1	0	open–open	TPSSh	M1	0	open–open
	M1-D3	0	open–open		M1-D3	0	open–open
TPSS-D4	M1	0	open–open	TPSSh-D4	M1	0	open–open
	M1-D3	−14	half-stacked		M1-D3	−14	half-stacked
ωB97M-V	M1	0	open–open	M06-2X	M1	0	open–open
	M1-D3	−43	stacked		M1-D3	−10	half-stacked
ωB97X-D	M1	0	open–open	M06-2X-D4	M1	0	open–open
	M1-D3	0	open–open		M1-D3	−12	half-stacked
BP86/RPA	M1	0	open–open	MP2	M1	0	half-stacked
	M1-D3	−17	stacked		M1-D3	−43	stacked

IV. Decomposition of the D3(BJ) energy corrections

As the major structural change observed upon inclusion of dispersion corrections was the stacking of the PLN ligands in the M1-D3 structure, a more detailed analysis of the en-

ergy contributions in this configuration was accomplished for one of the complexes, namely $[Eu(PLN)_4Ca]^+$. The energy breakdown is summarized in Figure 4, where the different contributions to the interaction dispersion energy, $\Delta E^{Disp}_{\mathrm{D3(BJ)}}$, were evaluated as follows:

$$\Delta E^{Disp}_{\mathrm{D3(BJ)}} = E^{Disp}_{\mathrm{D3(BJ)}}(\text{M2-D3}) - E^{Disp}_{\mathrm{D3(BJ)}}(\text{M1-D3}). \quad (1)$$

The decomposition was carried out in four steps. Starting from the whole complex (step 0) parts were gradually removed in consecutive steps to see where the D3(BJ) correction contributes the most. At the beginning (for the whole complex) the energy difference $\Delta E_{\mathrm{D3(BJ)}}$ is 175 kJ mol^{-1} and it does not change considerably when the Ca atom is removed (183 kJ/mol) (step 1). In a second step, the Eu atom is abstracted with a slight change of the dispersion contribution (170 kJ/mol). In the next step (step 3), one of the PLN ligands was taken out and we observe a significant drop in $\Delta E_{\mathrm{D3(BJ)}}$ to values of $\approx$ 80–90 kJ/mol. This can be attributed to the breaking of one of the stacked PLN ligand pairs in the M1-D3 structure. The energy range is due to the fact that different PLN ligands can be chosen to be removed in both structures giving a range of possible values rather than a single one. In the last step, there exist two qualitatively different options: to remove the "unpaired" PLN ligand so that a stacked structure remains in M1-D3 with an energy difference of $\Delta E_{\mathrm{D3(BJ)}} \approx 90$ kJ/mol (Step 4a in Figure 4) or to get rid of one of the "paired" PLN ligands such that no stacked structure remains (Step 4b in Figure 4). In the latter case, both residual structures are essentially isoenergetic ($\Delta E_{\mathrm{D3(BJ)}} \approx$ 0–5 kJ/mol). This analysis confirms the expectations that the energetic gain associated with the use of D3(BJ) corrections for the complex structures is primarily due to the stacking of PLN groups. Therefore it seems worthwhile exploring in detail the interaction between two PLN ligands.

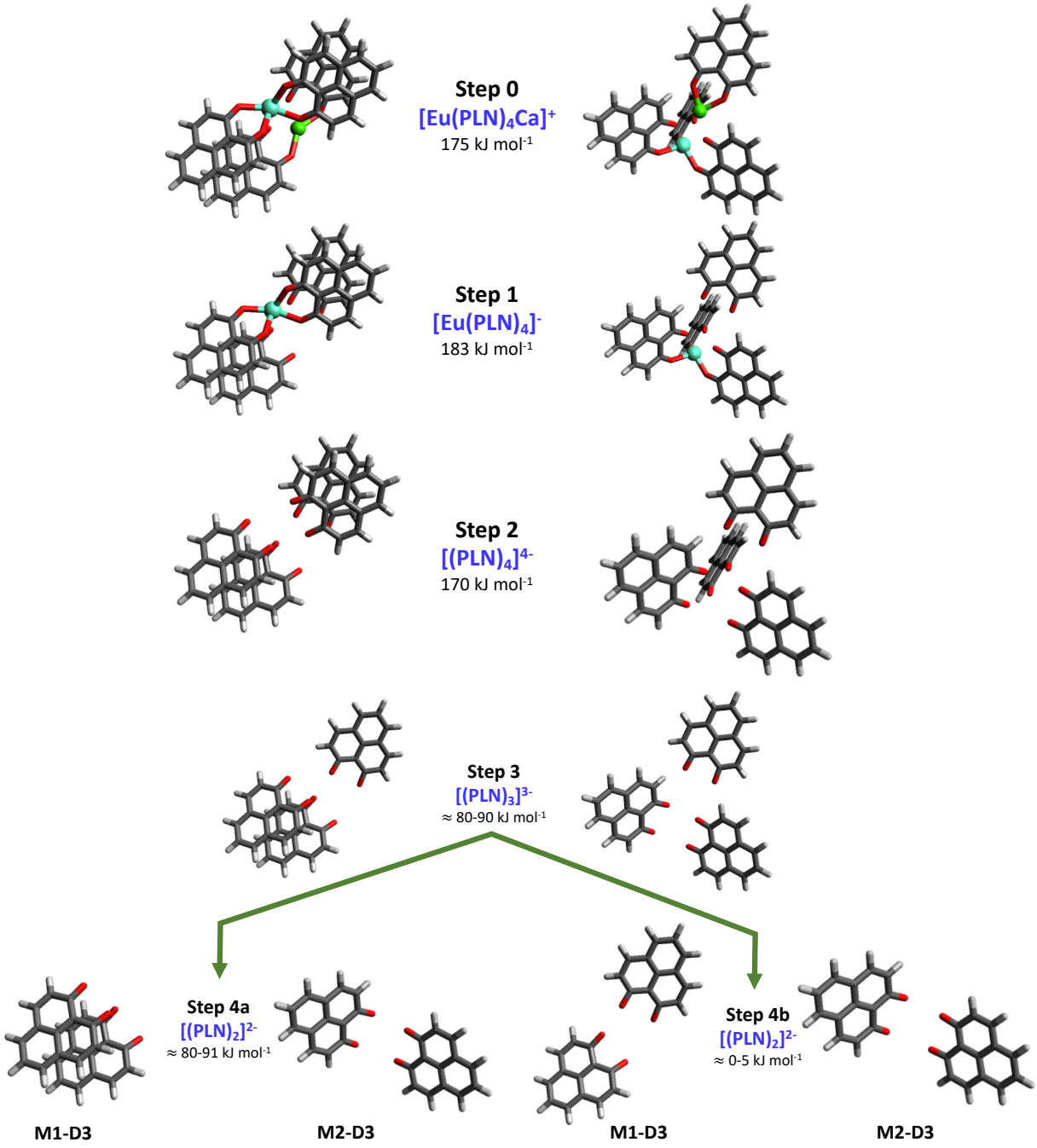

Figure 4: Energy decomposition of M1-D3 (left) and M2-D3 (right) for $[Eu(PLN)_4Ca]^+$ complex ($\Delta E_{D3(BJ)}$, see text for definition). The charge is left out in the description as it is not important since the D3(BJ) correction only takes into account positions of atoms (europium: clear blue; calcium: green; oxygen: red).

V. Basis set assessment

The def2-TZVPP[5] basis set was employed along all this study, however, in order to assess the adequacy of this basis set for the explicitly correlated calculations (F12)[6] a comparative study between the def2-TZVPP and cc-pVTZ-F12[7,8] basis sets employing various methods with and without F12 corrections was carried out on three different configurations of the benzene dimer (see Figure 5).

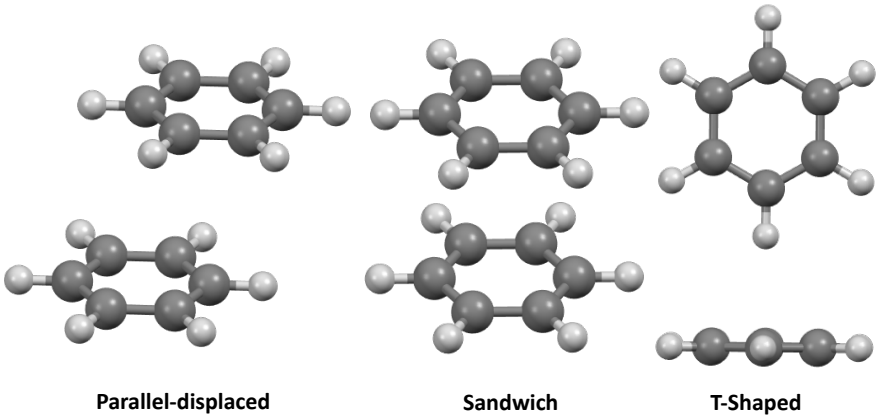

Figure 5: Parallel-displaced, sandwich and T-shaped configuration of the benzene dimer.

In the case of benzene dimers, the interaction energy was calculated according to the expression: $\Delta E_{(C_6H_6)_2} = E_{(C_6H_6)_2} - 2E_{(C_6H_6)}$. In the present work all the calculations were based on geometries computed at the CCSD(T)/aug-cc-pVQZ level taken from Reference 9. As can be seen in Table 3, for the three conformations of the benzene dimer, regardless of whether the basis set was optimized with explicitly correlated F12 methods or not, the same interaction energies (only 1 kJ mol^{-1} of discrepancy) were obtained. In the case of Ligandpair12 and Ligandpair34, the tests carried out using second-order perturbation theory with and without explicit correlation F12 also show that the differences obtained with both base sets amount to only 1 kJ mol^{-1}. With these results, the use of the def2-TZVPP basis function was justified for the benchmarking study on Ligandpair12 and Ligandpair34.

Table 3: Interaction energy for the benzene dimer ($\Delta E_{(C_6H_6)_2}$) and Ligandpair12 (ΔE_{12}) and Ligandpair34 (ΔE_{34}) obtained with different methods and basis sets (Units: kJ mol^{-1}).

	Parallel-Displaced		**Sandwich**		**T-Shaped**	
	def2-TZVPP	cc-pVTZ-F12	def2-TZVPP	cc-pVTZ-F12	def2-TZVPP	cc-pVTZ-F12
MP2[a]	-20	-20	-14	-14	-16	-16
MP2(F12)[a]	-19	-19	-13	-13	-15	-15
MP2/aug-cc-pVTZ	-19		-14		-14	
MP2/aug-cc-pVQZ	-20		-14		-15	
CCSD[a]	-8	-8	-4	-4	-10	-10
CCSD(F12*)[a,b]	-7	-7	-3	-3	-9	-9
CCSD(T)[a]	-12	-12	-8	-8	-12	-12
CCSD(F12*)(T)[a,b]	-12	-11	-7	-7	-12	-12
CCSD(T)/aug-cc-pVQZ	-11		-7		-11	
CBS CCSD(T)[c]	-11		-8		-12	

	Ligandpair12			**Lingadpair34**		
	def2-TZVPP	cc-pVTZ-F12	$\Delta E_{\text{TZVPP-TZF12}}$	def2-TZVPP	cc-pVTZ-F12	$\Delta E_{\text{TZVPP-TZF12}}$
MP2	-93	-88	-5	-91	-85	-6
MP2(F12)	-86	-82	-4	-85	-80	-5
$\Delta E_{\text{MP2-MP2(F12)}}$	-7	-5		-6	-5	

[a] Starting geometry obtained at the CCSD(T)/aug-cc-pVQZ (all g functions on carbon and all f functions on hydrogen were excluded. Taken from Ref. 9.

[b] CCSD(F12*) method explained in Ref. 10.

[c] At the MP2/aug-cc-pVTZ optimized dimer geometry. Table 2 of Ref. 9.

VI. Study of the Ligandpair34

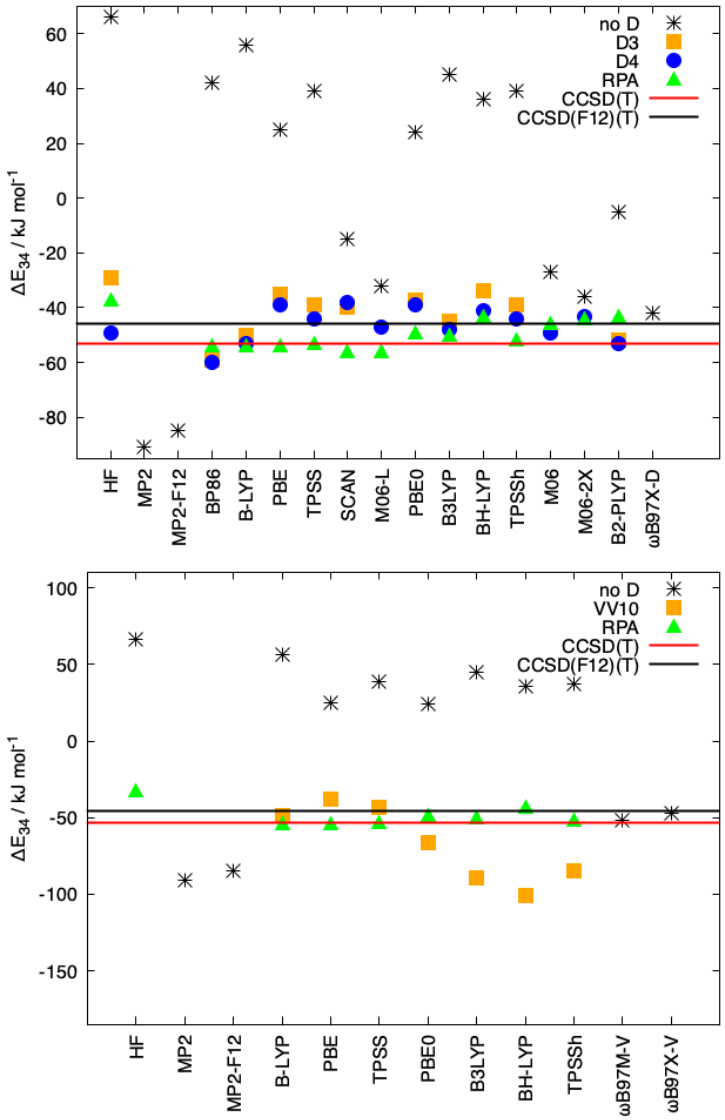

Figure 6: Interaction energies ΔE_{34} for Ligandpair34, obtained with different functionals and with London dispersion corrections using the models D3(BJ) and D4 (top), the model VV10 (bottom), as well as applying the random phase approximation (RPA). Reference values calculated at the CCSD(T) and CCSD(F12)(T) levels are also displayed. The def2-TZVPP basis set was used in all cases.

VII. Study of the metal coordination

Table 4: Fractional coordination numbers (fCN) for calcium and europium and dispersion energies (E_{Disp}) for the Eu-Ca pair as well as the total molecule. (Normal font used for values obtained with DFT-D3(BJ), values in brackets and cursive were calculated with DFT-D4. All computations were performed with the def2-TZVPP basis set.)

Method	Starting point	Type of structure	fCN(Ca)	fCN(Eu)	E_{Disp}(Eu-Ca) kcal mol^{-1}	E_{Disp}(Total) kcal mol^{-1}
BP86	M1	open-open	7.1 *(4.8)*	7.7 *(5.2)*	-1.566 *(-0.307)*	-163.38 *(-164.83)*
	M1-D3	open-open	7.1 *(4.8)*	7.7 *(5.3)*	-1.567 *(-0.307)*	-163.35 *(-164.82)*
BP86-D3(BJ)	M1	stacked	7.3 *(5.0)*	8.0 *(5.5)*	-1.566 *(-0.270)*	-204.77 *(-188.44)*
	M1-D3	stacked	7.3 *(5.0)*	8.0 *(5.5)*	-1.570 *(-0.270)*	-204.78 *(-188.46)*
BP86-D4	M1	stacked	7.0 *(5.1)*	8.1 *(5.5)*	-1.571 *(-0.270)*	-203.7 *(-187.77)*
	M1-D3	stacked	7.4 *(5.1)*	8.1 *(5.6)*	-1.571 *(-0.270)*	-203.71 *(-187.78)*
BLYP	M1	open-open	7.0 *(4.7)*	7.6 *(5.1)*	-1.463 *(-0.332)*	-201.53 *(-217.72)*
	M1-D3	open-open	6.9 *(4.7)*	7.6 *(5.1)*	-1.463 *(-0.332)*	-201.5 *(-217.70)*
BLYP-D3(BJ)	M1	open-open	7.0 *(4.7)*	7.8 *(5.3)*	-1.462 *(-0.331)*	-206.36 *(-222.88)*
	M1-D3	stacked	7.2 *(4.9)*	7.8 *(5.4)*	-1.466 *(-0.331)*	-241.00 *(-259.32)*
BLYP-D4	M1	half-stacked	7.3 *(5.0)*	7.9 *(5.4)*	-1.467 *(-0.331)*	-225.00 *(-242.84)*
	M1-D3	stacked	7.3 *(5.0)*	7.9 *(5.4)*	-1.467 *(-0.331)*	-243.51 *(-262.74)*
PBE	M1	open-open	7.1 *(4.8)*	7.7 *(5.2)*	-0.523 *(-0.184)*	-96.16 *(-105.20)*
	M1-D3	open-open	7.1 *(4.8)*	7.7 *(5.2)*	-0.523 *(-0.184)*	-96.20 *(-105.24)*
PBE-D3(BJ)	M1	open-open	7.1 *(4.8)*	7.8 *(5.3)*	-0.523 *(-0.183)*	-97.42 *(-106.60)*
	M1-D3	half-stacked	7.5 *(5.1)*	7.9 *(5.4)*	-0.523 *(-0.183)*	-105.62 *(-116.05)*
PBE-D4	M1	open-open	7.2 *(4.9)*	7.9 *(5.3)*	-0.523 *(-0.183)*	-97.68 *(-107.00)*
	M1-D3	half-stacked	7.3 *(5.0)*	8.0 *(5.5)*	-0.526 *(-0.183)*	-119.61 *(-131.6)*
TPSS	M1	open-open	7.1 *(4.8)*	7.8 *(5.3)*	-0.753 *(-0.227)*	=124.46 *(-140.66)*
	M1-D3	open-open	7.1 *(4.8)*	7.8 *(5.3)*	-0.497 *(-0.190)*	-124.44 *(-140.65)*
TPSS-D3(BJ)	M1	open-open	7.2 *(4.9)*	7.9 *(5.4)*	-0.753 *(-0.226)*	-126.79 *(-143.26)*
	M1-D3	stacked	7.3	8.1	-0.393	-150.56

			(5.0)	*(5.5)*	*(-0.259)*	*(-169.47)*
TPSS-D4	M1	open-open	7.6	8.1	-0.753	-140.75
			(5.2)	*(5.5)*	*(-0.226)*	*(-159.22)*
	M1-D3	half-stacked	7.4	8.1	-0.753	-153.44
			(5.1)	*(5.6)*	*(-0.227)*	*(-173.11)*
PBE0	M1	open-open	7.1	8.0	-0.595	-89.27
			(4.9)	*(5.5)*	*(-0.159)*	*(-93.65)*
	M1-D3	open-open	7.2	8.0	-0.595	-89.28
			(4.9)	*(5.5)*	*(-0.159)*	*(-93.67)*
PBE0-D3(BJ)	M1	open-open	7.2	8.1	-0.595	-90.62
			(4.9)	*(5.5)*	*(-0.159)*	*(-95.12)*
	M1-D3	half-stacked	7.6	8.2	-0.594	-99.34
			(5.2)	*(5.6)*	*(-0.159)*	*(-104.77)*
PBE0-D4	M1	open-open	7.2	8.1	-0.595	-90.87
			(4.9)	*(5.5)*	*(-0.159)*	*(-95.47)*
	M1-D3	half-stacked	7.6	8.3	-0.594	-99.75
			(5.2)	*(5.7)*	*(-0.159)*	*(-105.32)*
B3LYP	M1	open-open	7.1	7.9	-0.137	-168.32
			(4.8)	*(5.4)*	*(-0.307)*	*(-166.21)*
	M1-D3	open-open	7.1	7.9	-1.370	-168.31
			(4.8)	*(5.4)*	*(-0.307)*	*(-197.3)*
B3LYP-D3(BJ)	M1	open-open	7.1	8.0	-1.371	-171.2
			(4.8)	*(5.4)*	*(-0.306)*	*(-169.33)*
	M1-D3	stacked	7.3	8.2	-1.371	-194.41
			(5.0)	*(5.6)*	*(-0.306)*	*(-194.60)*
B3LYP-D4	M1	open-open	7.1	8.0	-1.371	-171.99
			(4.9)	*(5.5)*	*(-0.306)*	*(-170.36)*
	M1-D3	stacked	7.4	8.3	-1.372	-196.62
			(5.1)	*(5.7)*	*(-0.306)*	*(-197.3)*
BHLYP	M1	open-open	7.2	8.0	-1.906	-136.22
			(4.9)	*(5.4)*	*(-0.518)*	*(-130.29)*
	M1-D3	open-open	7.1	7.9	-1.371	-168.31
			(4.8)	*(5.4)*	*(-0.307)*	*(-166.21)*
BHLYP-D3(BJ)	M1	open-open	7.2	8.1	-1.904	-137.72
			(4.9)	*(5.5)*	*(-0.517)*	*(-132.01)*
	M1-D3	half-stacked	7.6	8.2	-1.899	-148.00
			(5.2)	*(5.6)*	*(-0.517)*	*(-144.26)*
BHLYP-D4	M1	open-open	7.3	8.1	-1.905	-138.26
			(4.9)	*(5.5)*	*(-0.517)*	*(-132.77)*
	M1-D3	half-stacked	7.6	8.3	-1.900	-148.82
			(5.2)	*(5.7)*	*(-0.517)*	*(-145.38)*
TPSSh	M1	open-open	7.1	7.9	-0.747	-118.03
			(4.8)	*(5.4)*	*(-0.197)*	*(-130.66)*
	M1-D3	open-open	7.1	7.9	-0.747	-118.04
			(4.8)	*(5.4)*	*(-0.197)*	*(-130.68)*
TPSSh-D3(BJ)	M1	open-open	7.2	8.0	-0.747	-120.58
			(4.9)	*(5.5)*	*(-0.197)*	*(-133.44)*
	M1-D3	stacked	7.4	8	-0.747	-140.03
			(5.1)	*(5.7)*	*(-0.196)*	*(-154.53)*
TPSSh-D4	M1	half-stacked	7.5	8.4	-0.747	-136.7
			(5.1)	*(5.8)*	*(-0.196)*	*(-151.37)*
	M1-D3	stacked	7.5	8.2	-0.748	-145.85
			(5.1)	*(5.7)*	*(-0.197)*	*(-161.08)*

References

(1) Greisch, J.-F.; Chmela, J.; Harding, M. E.; Wunderlich, D.; Schäfer, B.; Ruben, M.; Klopper, W.; Schooss, D.; Kappes, M. M. Correlation of the structural information obtained for europium-chelate ensembles from gas-phase photoluminescence and ion-mobility spectroscopy with density-functional computations and ligand-field theory. *Phys. Chem. Chem. Phys.* **2017**, *19*, 6105.

(2) Burns, L.; Vázquez-Mayogoitia, A.; Sumpter, B.; Sherrill, C. Density-functional approaches to noncovalent interactions: A comparison of dispersion corrections (DFT-D), exchange-hole dipole moment (XDM) theory, and specialized functionals. *J. Chem. Phys.* **2011**, *134*, 084107.

(3) Campuzano, I.; Bush, M. F.; Robinson, C. V.; Beaumont, C.; Richardson, K.; Kim, H.; Kim, H. I. Structural characterization of drug-like compounds by ion mobility mass spectrometry: comparison of theoretical and experimentally derived nitrogen collision cross sections. *Anal. Chem.* **2012**, *84*, 1026.

(4) Siu, C.-K.; Guo, Y.; Saminathan, I.; Hopkinson, A. C.; Siu, K. W. M. Optimization of parameters used in algorithms of ion-mobility calculation for conformational analyses. *J. Phys. Chem. B* **2010**, *114*, 1204.

(5) Weigend, F.; Ahlrichs, R. Balanced basis sets of split valence, triple zeta valence and quadruple zeta valence quality for H to Rn: Design and assessment of accuracy. *Phys. Chem. Chem. Phys.* **2005**, *7*, 3297.

(6) Hättig, C.; Klopper, W.; Köhn, A.; Tew, D. P. Explicitly correlated electrons in molecules. *Chem. Rev.* **2012**, *112*, 4.

(7) Peterson, K. A.; Adler, T. B.; Werner, H.-J. Systematically convergent basis sets for explictly correlated wavefunctions: the atoms H, He, B-Ne, and Al-Ar. *J. Chem. Phys.* **2008**, *128*, 084102.

(8) Hill, J. G.; Peterson, K. A. Correlation consistent basis sets for explicitly correlated wavefunctions: valence and core-valence basis sets for Li, Be, Na and Mg. *Phys. Chem. Chem. Phys.* **2010**, *12*, 10460.

(9) Sinnokrot, M. O.; Sherrill, C. D. Highly acccurate coupled cluster potential energy curves for the benzene dimer: sandwich, T-shaped, and parallel-displaced configurations. *J. Phys. Chem. A* **2004**, *108*, 10200.

(10) Hättig, C.; Tew, D. P.; Köhn, A. Accurate and efficient approximations to explicitly correlated coupled-cluster singles and doubles, CCSD-F12. *J. Chem. Phys.* **2010**, *132*, 231102.